Journal of Organometallic Chemistry, 473 (1994) 175–186

Unusual reactivities of $(\mu\text{-}\eta^2\text{:}\eta^2\text{-FP–C}\equiv\text{C–H})Co_2(CO)_6$, the adducts of FP–C≡C–H to $Co_2(CO)_8$: photolysis, thermolysis and reduction with hydrosilanes giving polynuclear complexes, $(CP)_2Fe_2Co_3(\mu_5\text{-C=CH})(CO)_{10}$, $(\mu\text{-CH=CH})[(-\mu_3\text{-C})Co_3(CO)_9]_2$ and $CpFeCo_3(\mu\text{-C=CH}_2)(CO)_9$

Munetaka Akita, Masako Terada, Naomi Ishii, Hideki Hirakawa and Yoshihiko Moro-oka

Research Laboratory of Resources Utilization, Tokyo Institute of Technology, 4259 Nagatsuta, Midori-ku, Yokohama 227 (Japan)

(Received December 1, 1993; in revised form December 29, 1993)

Abstract

The properties and reactivities of $(\mu\text{-}\eta^2\text{:}\eta^2\text{-FP–C}\equiv\text{C–H})Co_2(CO)_6$ (**3**) [the FP–C≡C–H adducts to $Co_2(CO)_8$: **3a** (FP = Fp), **3b** (FP = Fp*)] have been compared with those of alkyne adducts $(\mu\text{-}\eta^2\text{:}\eta^2\text{-R–C}\equiv\text{C–R})Co_2(CO)_6$ and the Ph analogue $(\mu\text{-}\eta^2\text{:}\eta^2\text{-Fp–C}\equiv\text{C–Ph})Co_2(CO)_6$ (**5**). Compound **3** has been shown to serve as a building block for polynuclear complexes. ^{13}CO-labelling experiments on **3a** and **5** have revealed an intramolecular exchange between the Fe–CO and Co–CO ligands. Photolysis of **3a, b** produces pentanuclear clusters $(CP)_2Fe_2Co_3(\mu_5\text{-C=CH})(CO)_{10}$ (**11a,b**), respectively, via an apparent addition reaction of a $(CP)FeCo(CO)_n$ fragment to **3**. On the other hand, thermolysis of **3a** gives the Fe-free hexacobalt cluster compound $(\mu\text{-CH=CH})[(-\mu_3\text{-C})Co_3(CO)_9]_2$ (**13**) which consists of two alkylidyne tricobalt units linked by the CH=CH bridge, whereas **3b** is thermolyzed to give the Fe–Co dimer without the C_2H ligand, $Cp^*Fe(CO)(\mu\text{-CO})_2Co(CO)_3$ (**14**), in addition to the photolysis product **11b**. Reduction of **3** with hydrosilanes gives a mixture containing 1,2-disilylethylene (**16**) and the tetranuclear μ-vinylidene cluster $CpFeCo_3(\mu_4\text{-C=CH}_2)(CO)_9$ (**12**) formally by way of hydrosilylation and hydrometallation (with a $HCo(CO)_n$ species) of the C_2H ligand, respectively. In the case of the Pauson-Khand reaction and catalytic cyclotrimerization **3a** exhibits reactivities similar to alkyne adducts to give the tricyclic cyclopentenone derivatives **18** (from norbornene and norbornadiene) and triphenylbenzenes, respectively.

Key words: Iron; Cobalt; Carbonyl; Polynuclear

1. Introduction

We have been studying [1] the syntheses and reactivities of polynuclear complexes derived from parent iron acetylides, the ethynyl complexes FP–C≡C–H (**1a**: FP = Fp; **1b**: FP = Fp*) and the ethynediyl complex Fp*–C≡C–Fp* (**2**). It is expected that regarding the coordination structure and reactivity the resulting polynuclear complexes containing C_2H_n ligands ($n = 0$, 1) of simple composition should serve as better model compounds for surface-bound hydrocarbyl species than C_2R complexes derived from alkynyl complexes bearing an organic group such as Ph, CO_2R and alkyl [2].

Treatment of the C_2H_n complexes **1** and **2** with dinuclear species such as $Co_2(CO)_8$ [1d], $Cp_2Ni_2(CO)_2$ [1e] and $Cp_2Mo_2(CO)_4$ [1h] successfully produces adducts in a manner similar to the reaction of alkynes (Scheme 1) [3]. Although the structure of most of the resulting adducts is similar to that of alkyne adducts $(\mu\text{-}\eta^2\text{:}\eta^2\text{-R–C}\equiv\text{C–R})M_2$ with a tetrahedral C_2M_2 core, the FP part often induces unusual properties which have not been observed for alkyne adducts. For example, the Mo adducts show fluxional behaviour by way of a vinylidene intermediate [1h] and the tetranuclear complex **4** where the $FeCo_2$ cluster unit and the Fp* group are linked by the C_2 bridge has proved also to

Correspondence to: Dr. M. Akita, Dr. Y. Moro-oka.

* Abbreviations used in this paper are as follows, CP: $\eta^5\text{-}C_5H_5$(Cp), $\eta^5\text{-}C_5Me_5$ (Cp*). FP: $CpFe(CO)_2$(Fp), $Cp^*Fe(CO)_2$(Fp*).

0022-328X/94/$7.00
SSDI 0022-328X(94)24422-F

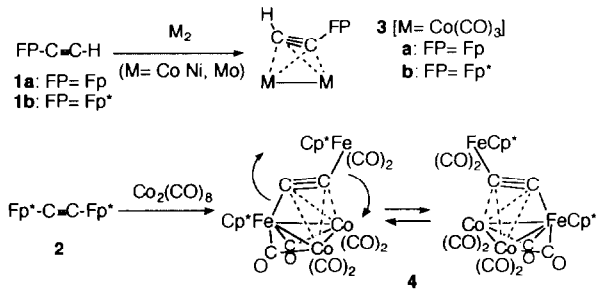

Scheme 1.

be fluxional via reversible metal–metal bond cleavage and recombination processes as revealed by variable temperature ^{13}C-NMR (Scheme 1) [1d]. In this paper we report some unusual properties and reactivities of the Co adducts **3a** and **3b**, in particular, formation and structure determination of higher-nuclearity cluster compounds.

2. Results and discussion

2.1. ^{13}CO-scrambling between Fe and Co centres in (μ-η^2:η^2-Fp–C≡C–R)$Co_2(CO)_6$ (3a) (R = H) and 5 (R = Ph)

Reaction of **1a** with $Co_2(CO)_8$ gave the adduct **3a** (Scheme 1), which, on treatment with hydrosilane, afforded a reduced organic product (see below). To determine the source of the C of the reduced product, ^{13}CO-enriched samples of **3a** were prepared. When a benzene solution of **3a** was exposed to ^{13}CO, both of the Fe and Co sites were enriched by ^{13}CO as determined by ^{13}C-NMR [Figs. 1a and b; eqn. (1) (*CO denotes the site enriched by ^{13}CO)].

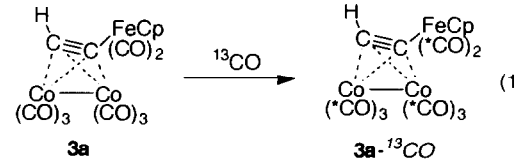

The estimated distribution of ^{13}CO (Fe–^{13}CO : Co–^{13}CO = 1 : 2.5) was roughly comparable to the number of the CO ligands (2 : 6), and incorporation of the ^{13}CO was also confirmed by red-shift of the ν(C≡O) absorptions. Because neither decomposed product nor the starting compound **1a** could be detected at all by the NMR analyses (Fig. 1(a) shows the spectrum of a reaction mixture after removal of the volatiles), incorporation of ^{13}CO appeared to proceed via a dissociative mechanism rather than via an associative mechanism. These results could be explained in terms of either CO exchange at both the Fe and Co sites (path i) or incorporation of external CO into either the Fe or Co site (path ii or iii) followed by intramolecular CO exchange (path iv) (Scheme 2). In order to check the second mechanism, reaction between **1a** and ^{13}CO-enriched $Co_2(CO)_8$ was carried out (eqn. (2)).

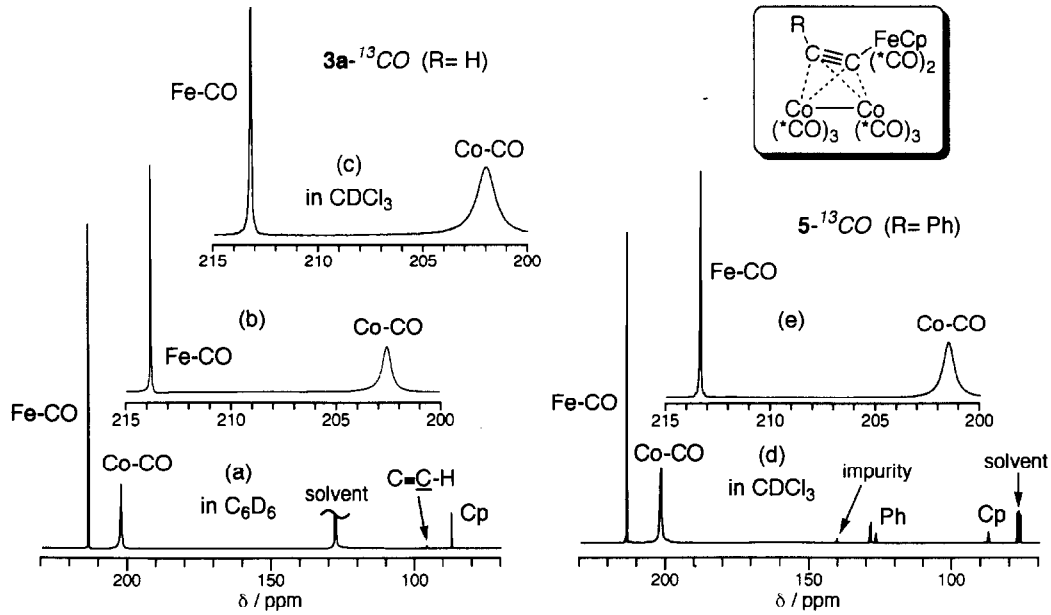

Fig. 1. ^{13}C-NMR spectra of ^{13}CO-enriched samples of **3a** and **5**: (a) a reaction mixture of **3a** treated with ^{13}CO (in C_6D_6; eqn. 1); (b) an expanded chart of the CO region of (a); (c) the CO region of **3a** obtained by treatment of **1a** with ^{13}CO-enriched $Co_2(CO)_8$ (in $CDCl_3$; eqn. 2); (d) ^{13}C-NMR spectrum of **5** obtained by treatment of Fp–C≡C–Ph with ^{13}CO-enriched $Co_2(CO)_8$ (in $CDCl_3$; eqn. 2); (e) an expanded chart of the CO region of (d).

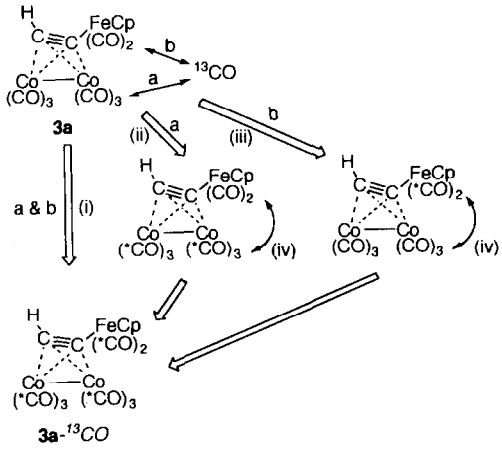

Scheme 2.

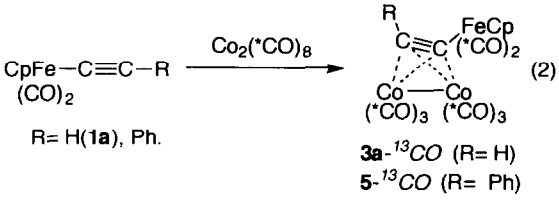

As a result, the ^{13}C-NMR spectrum of the product (Fig. 1(c)) which was essentially identical to Figs. 1(a),(b) verified the participation of the intramolecular CO-scrambling process (path iv in Scheme 2). Because under similar reaction conditions (2 atm at ambient temperature) $Co_2(CO)_8$ incorporated ^{13}CO but **2** did not, initial ^{13}CO-uptake at the Co-site and subsequent intramolecular CO transfer between Fe and Co (path ii and then iv) appear to be the most likely process for the ^{13}CO-scrambling. The intermolecular CO exchange reaction of $(\mu\text{-}\eta^2\text{:}\eta^2\text{-R-C}\equiv\text{C-R})Co_2(CO)_6$ has already been reported by Cetini *et al.*, who also revealed that the reaction rate of the complex with a more electron donating substituent (R) was faster [4]. Although, according to path iv, coalescence of the Fe–CO and Co–CO signals at higher temperature was expected, any notable change of the ^{13}CO-NMR spectra was not observed up to 80°C (at 67 MHz). Above 80°C **3a** gradually decomposed as described below. Because a similar CO exchange process was observed for **5** (the Ph analogue of **3a**) as confirmed by the reaction between Fp–C≡C–Ph and ^{13}CO-enriched $Co_2(CO)_8$ (Figs. 1(d),(e); eqn. (2)), the present phenomenon may be a general one observed for this class of compounds. The CO-exchange may take place at the stage of a transient 56e-*arachno* pentagonal bipyramidal intermediate **6** with Fe–Co bonds (see below) [5] as in the case of the fluxional process of **4** [1d].

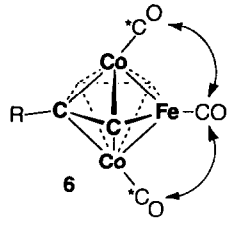

To confirm the initial reaction site of the ligand exchange, reaction of **2** with PPh_3 was examined. Treatment of **3a** with a slight excess of PPh_3 readily produced a PPh_3-derivative (eqn. (3)).

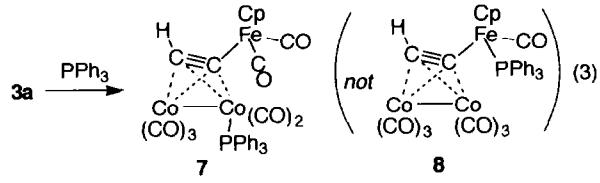

Although, unfortunately, a pure sample could not be obtained due to thermal instability, the product was assigned to **7** where one of the Co–CO ligands in **3a** was substituted by PPh_3 on the basis of the following spectroscopic data: (1) the retention of the tetrahedral C_2Co_2 core was indicated by the $C_\beta\equiv C_\alpha H$ resonances [$\delta_C(C_\alpha)$ 97.6 ($J(^{13}C\text{-}^{31}P) = 3.7$ Hz, $^1J(^{13}C\text{-}^1H) = 209.6$ Hz); $\delta_C(C_\beta)$ 101.9 ($J(^{13}C\text{-}^{31}P) = 7.3$ Hz, $^2J(^{13}C\text{-}^1H) = 11.0$ Hz)] which were close to those of the starting compound **3a** [$\delta_C(C_\beta)$ 95.7 ($^1J(^{13}C\text{-}^1H) = 209.6$ Hz); $\delta_C(C_\alpha)$ 102.2 ($^2J(^{13}C\text{-}^1H) = 11.0$ Hz)]; (2) the comparable $J(^{13}C\text{-}^{31}P)$ values for the C_α and C_β signals preferred **7** over another possible isomer **8** which should show considerably different $^1J(^{13}C\text{-}^{31}P)$ and $^2J(^{13}C\text{-}^{31}P)$ (24 Hz) for the Fe–CO signal might support **8**, the ^1H-decoupled ^{31}P-NMR signal of ^{13}CO-enriched **7** appeared as a broad signal rather than as a superposition of a singlet and a doublet signal which was expected for **8**. Therefore the doublet CO signal might be due to $^4J(^{13}C\text{-}^{31}P)$. In addition, the ^1H- and ^{13}C-NMR signals of the Cp ligand appeared as singlets without coupling with the ^{31}P-nucleus, and this regiochemistry is supported by the structure of the Pauson-Khand reaction products (see below) where the Fp structure was retained. Replacement of a CO ligand by PPh_3 was already reported for alkyne adducts, but it required more vigorous conditions (heating at 60°C) [6]. The higher reactivity of **3a** may result from the better electron-donating ability of Fp–C≡C–H, as is consistent with Cetini's work.

2.2. *Photolysis and thermolysis of 3a,b giving higher-nuclearity cluster compounds*

Two decades ago Yamazaki *et al.* reported the synthesis of analogues of **3a**, $[\mu\text{-}\eta^2\text{:}\eta^2\text{-CpFe(CO)L-C}\equiv\text{C-}$

R]$Co_2(CO)_6$ (**9**) (R = Me, Ph; L = CO, PMe_2Ph) (Scheme 3) [7], and the structure of **5** (R = Ph; L = CO) later determined by Bruce *et al.* was very close to that of **3a** [8]. Yamazaki *et al.* also found that thermolysis of **9** resulted in loss of two CO ligands to give cluster compounds **10**, the proposed core structure of which was very similar to that of **4** [1d]. **10** should be formed by decarbonylation and subsequent compensation of the coordinative unsaturation by formation of metal–metal bonds with bridging CO. Taking into account these results, photolysis and thermolysis of **3** were examined.

Photolysis of **3a** and **3b** in benzene gave new complexes **11a** and **11b** as predominant products, respectively, which were readily isolated as black crystals after simple crystallization (eqn. (4)).

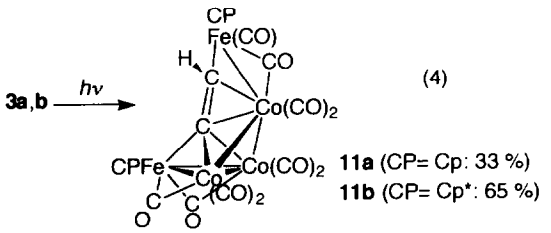

(4)

No other byproduct except for very small amounts of Fp_2 and Fp_2^* was detected by ^{1}H-NMR and TLC. The NMR analyses of **11** revealed the presence of two Cp(Cp*) ligands in different environments in addition to a C_2H ligand. The C_2H NMR parameters and patterns of the ν(CO) absorptions of **11a,b** were very

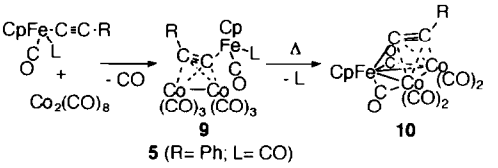

Scheme 3.

similar to each other, and the highly deshielded quartemary carbon signals [δ_C 306.7 (**11a**), 310.0 (**11b**)] suggested that the C_2H ligands were located in polymetallic environments [9]. Then the molecular structure of **11a** was determined by X-ray crystallography. The crystallographic data and selected structural parameters are summarized in Tables 1 and 2, and the molecular structure and core structures are reproduced in Figs. 2 and 3. As expected from the ^{13}C-NMR spectrum, **11a** proved to be a pentanuclear cluster compound bearing the multiply bridging C_2H ligand, $Cp_2Fe_2Co_3(\mu_5$-C=CH)$(CO)_{10}$. The Fe_2Co_3 skeleton adopts a spiked butterfly structure, that is, the core skeleton comprising of Fe1 and Co1 ~ 3 adopts a butterfly structure and C1 lies approximately equidistant from the four metal centres [1.92(1) ~ 2.09(1) Å] as can be seen from side and top views of the $Fe_2Co_3(\mu_5$-C=CH) core structure (Fig. 3). However, the π-coordination of the C1–C2 part to Co3 results in considerable elongation of the C1–Co3 distance compared with the C1–Fe1 distance. Thus the photolysis product **11a** can be viewed as a derivative of the tetranuclear bridg-

TABLE 1. Crystallographic data for **11a**, **13**, **14** and **18**

	11a	**13**	**14**	**18**
formula	$C_{32}H_{11}O_{10}Fe_2Co_3$	$C_{22}H_2O_{18}Co_6$	$C_{16}H_{15}O_6FeCo$	$C_{17}H_{12}O_3Fe$
fw	843.93	907.84	418.07	320.13
space group	$P2_1/c$	$P\bar{1}$	$P\bar{1}$	$P2_1/n$
a/Å	16.819(8)	8.868(2)	9.231(3)	6.952(6)
b/Å	8.618(1)	12.270(2)	12.225(3)	20.061(19)
c/Å	16.625(4)	8.119(3)	8.264(4)	10.467(11)
α/deg	90	104.76(2)	90.52(3)	90
β/deg	98.41(3)	114.06(2)	110.58(3)	105.72(7)
γ/deg	90	95.38(2)	90.64(2)	90
V/Å^3	2384(2)	760.3(4)	872.9(5)	1405(2)
Z	4	1	2	4
d_{calcd}/g · cm^{-3}	2.35	1.98	1.59	1.51
μ/cm^{-1}	33.0	32.7	18.0	10.8
2θ/deg	2–55	5–55	5–55	5–50
no. of data collecd	6018	3720	4244	2773
no. of data with $I > 3\sigma(I)$	3543	2300	2715	1184
no. of variables	334	212	217	190
R	0.075	0.023	0.031	0.068
R_w	0.081	0.032	0.045	0.043

TABLE 2. Selected structural parameters for **11a** [and **12**] [a]

Bond lengths (Å)					
C1–C2	1.41(1)	[1.43(1)]	Fe1–Co1	2.502(2)	[2.499(2)]
C1–Fe1	1.94(1)	[1.933(8)]	Fe1–Co2	2.532(2)	[2.499(2)]
C1–Co1	1.98(1)	[1.917(6)]	Fe2–Co3	2.548(3)	
C1–Co2	1.92(1)	[1.917(6)]	Co1–Co2	2.450(2)	[2.456(3)]
C1–Co3	2.09(1)	[2.087(8)]	Co1–Co3	2.629(3)	[2.581(3)]
C2–Fe2	2.01(1)		Co2–Co3	2.593(2)	[2.581(3)]
C2–Co3	2.00(1)	[2.09(1)]			
Bond angles (°)					
C2–C1–Fe1	136.1(8)		Fe1–Co1–Co2	61.49(7)	
C2–C1–Co1	117.6(7)		Fe1–Co1–Co3	100.30(8)	
C2–C1–Co2	138.9(8)		Co2–Co1–Co3	61.28(6)	
C2–C1–Co3	66.5(6)		C1–Co2–Fe1	49.4(3)	
Fe1–C1–Co1	79.3(4)		C1–Co2–Co1	52.2(3)	
Fe1–C1–Co2	82.0(4)		C1–Co2–Co3	52.7(3)	
Fe1–C1–Co3	155.5(6)		Fe1–Co2–Co1	60.26(7)	
Co1–C1–Co2	77.9(4)		Fe1–Co2–Co3	100.48(8)	
Co1–C1–Co3	80.4(4)		Co1–Co2–Co3	62.76(7)	
Co2–C1–Co3	80.5(4)		C1–Co3–C2	40.2(4)	
C1–C2–Fe2	122.8(8)		C1–Co3–Fe2	80.3(3)	
C1–C2–Co3	73.3(6)		C1–Co3–Co1	47.9(3)	
Fe2–C2–Co3	79.0(4)		C1–Co3–Co2	46.9(3)	
C1–Fe1–Co1	51.0(3)		C2–Co3–Fe2	50.6(3)	
C1–Fe1–Co2	48.6(3)		C2–Co3–Co1	76.6(3)	
Co1–Fe1–Co2	58.25(7)		C2–Co3–Co2	84.5(3)	
C2–Fe2–Co3	50.4(3)		Fe2–Co3–Co1	125.98(8)	
C1–Co1–Fe1	49.7(3)		Fe2–Co3–Co2	102.69(8)	
C1–Co1–Co2	50.0(3)		Co1–Co3–Co2	55.97(7)	
C1–Co1–Co3	51.6(3)				

[a] bond lengths shown in brackets are for **12** with mirror symmetry.

ing vinylidene cluster compound **12** (see below) which was prepared and structurally characterized by Stone

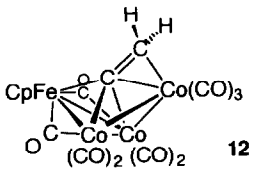

12

et al. [11]. The structure of **11a** corresponds to a structure where one of the methylene hydrogen atoms in the parent vinylidene complex **12** is replaced by the spiked Fe group (Fe2), which is further bonded to the wingtip Co atom (Co3) of the butterfly skeleton. In accord with this description, the bond lengths and the δ_C(C1) value of **11a** are comparable to those of **12** (the bond lengths are shown in Table 2; δ_C(C1) 304.3). However, owing to the Fe2–Co3 interaction the vinylidene ligand plane is considerably twisted [the torsion angle Fe1–C1–C2–Fe2 = 127.2(9)°] and C2 is tilted toward the Co1 side [*cf.* Co2–C1–C2 = 138.9(8)°, Co1–C1–C2 = 117.6(7)°]. In the case of **12**, the corresponding torsion angle is 60° and the two Co–C–C angles (130°) are equal because of the structure with a

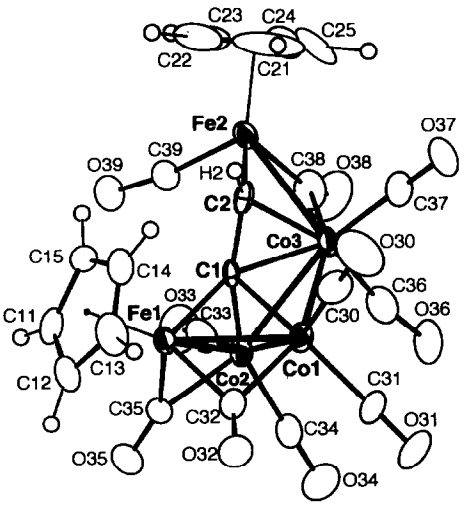

Fig. 2. Molecular structure of **11a** drawn at the 30% probability level.

mirror symmetry. The Cp* complex **11b** was assigned to the Cp* analogue of **11a** on the basis of the similar spectroscopic features as well as the FDMS data. This complex was also obtained by reaction between **2** and $Co_4(CO)_{12}$ instead of the adduct with an octahedral C_2Co_4 core [12]. In contrast to **3**, it was found that the tetranuclear μ_4-C_2 complex **4** was stable under photochemical reaction conditions.

Thermolysis of **3** also produced polynuclear complexes. Heating a benzene solution of **3a** at 90°C gave a mixture of products. Although a considerable amount of Fp_2 was detected as the sole Cp-containing product by the ^{1}H-NMR spectrum of a reaction mixture, a new red-purple compound **13** was isolated by chromatographic separation (eqn. (5)).

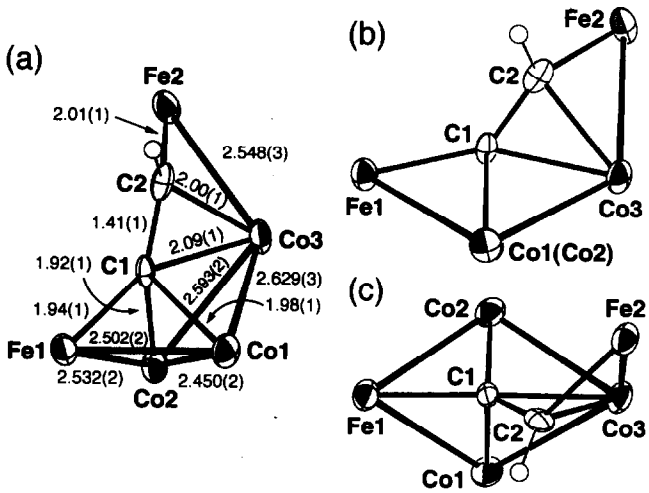

Fig. 3. Core structures of **11a**: (a) an overview; (b) a side view; (c) a top view.

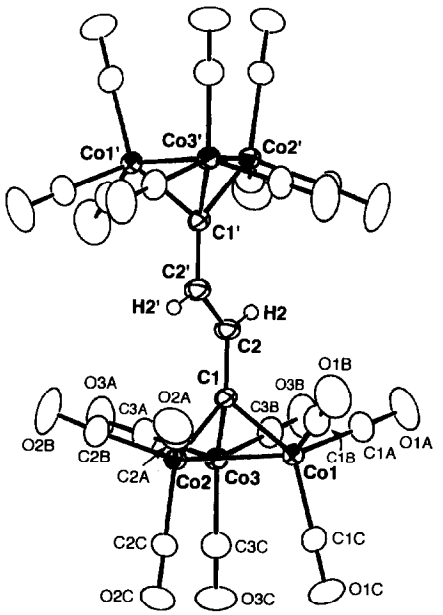

Fig. 4. Molecular structure of **13** drawn at the 30% probability level.

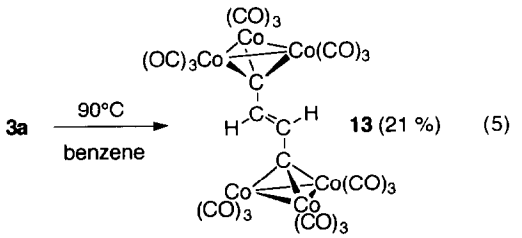

Interestingly, **13** contained no Cp ligand and spectroscopic analyses revealed merely the presence of an olefinic CH group [δ_H 7.96 (s); δ_C 150.0 (d, J = 154.3 Hz)] and CO ligands [ν(C≡O) 2027 cm^{-1}]. Then **13** was subjected to X-ray crystallographic analysis (Fig. 4; Tables 1 and 3). As a result, **13** proved to be composed of two tricobalt alkylidyne units linked by a CH=CH bridge, and possessed a centrosymmetric structure with respect to the midpoint of the C=C bond. In accord with this structure, the alkylidyne carbon atom signal could be located at δ_C 306.7. While the structural parameters concerning the tricobalt alkylidyne units fall in the normal range of related compounds [13] and the C=C length is comparable to alkenes (C=C: 1.34 Å), the C–CH= distance is substantially shorter than usual C(sp^3)–C(sp^2) lengths (1.50 Å) [14].

On the other hand, thermolysis of **3b** in benzene afforded a Cp*-containing product **14** along with the photolysis product **11b** (eqn. (6)).

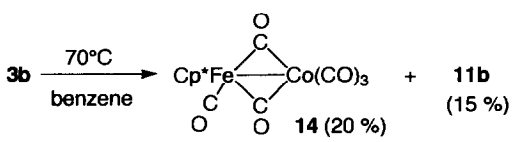

TABLE 3. Selected structural parameters for **13**

Bond lengths (Å)			
C1–C2	1.434(4)	Co1–Co2	2.4771(9)
C1–Co1	1.908(3)	Co1–Co3	2.4689(8)
C1–Co2	1.905(3)	Co2–Co3	2.466(1)
C1–Co3	1.918(3)	Co–CO_{eq} [a]	1.785(3)–1.795(4)
C2–C2′	1.331(6)	Co–CO_{ax} [b]	1.826(3)–1.834(3)
C2–H2	0.87(3)		
Bond angles (°)			
Co1–C1–Co2	81.0(1)	C2′–C2–H2	117(2)
Co1–C1–Co3	80.4(1)	Co2–Co1–Co3	59.82(3)
Co1–C1–C2	128.1(2)	Co1–Co2–Co3	59.93(3)
Co2–C1–Co3	80.3(1)	Co–Co–C1	49.42(8)–50.07(9)
Co2–C1–C2	134.2(2)	CO_{eq}–Co–CO_{eq} [a]	95.0(2)–97.8(2)
Co3–C1–C2	132.7(2)	CO_{eq}–Co–CO_{ax} [a,b]	97.6(1)–104.1(2)
C1–C2–C2′	127.7(4)	Co–C–O(CO)	176.8(4)–179.0(3)
C1–C2–H2	116(2)		

[a] CO_{eq}:CO ligands of A and B series. [b] CO_{ax}:CO ligands of C series.

Because NMR and IR spectra of **14** revealed only the presence of Cp*Fe(CO) and μ-CO functional groups and, more importantly, multiply bridging C_2 ligands often escaped from ^{13}C-NMR detection [1d,15], **14** was characterized by X-ray crystallography (Fig. 5 and Table 4). Contrary to our expectations, **14** turned out to be a simple Fe–Co dimer complex without C_2H_n ligand, Cp*Fe(CO)(μ-CO)$_2$Co(CO)$_3$. When the structure of **14** was compared with that of the previously reported Cp analogue, CpFe(CO)(μ-CO)$_2$Co(CO)$_3$ (**15**) (its structural parameters are shown in brackets in Table 4) [16], they were very similar to each other except for the following aspect. Because the structure of the Cp complex **15** has mirror symmetry with respect to the plane passing through Fe, Co, the centroid of the Cp ring and two terminal CO ligands corresponding to C1O1 and C4O4, the bridging mode of the two μ-CO ligands is the same and they are tilted toward Co [Fe–C: 1.882(7) Å, Co–C: 2.036(7) Å; Fe–C–O: 144.5(6)°, Co–

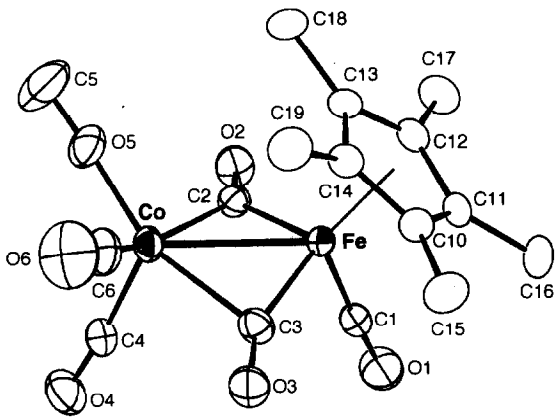

Fig. 5. Molecular structure of **14** drawn at the 30% probability level.

TABLE 4. Selected structural parameters for **14** [and **15**] [a]

Bond lengths (Å)			
Fe–Co	2.591(1) [2.545(1)]	C1–O1	1.143(4) [1.13(1)]
Fe–C1	1.762(3) [1.75(1)]	C2–O2	1.166(3) [1.147(8)]
Fe–C2	1.941(3) [1.882(7)]	C3–O3	1.145(4) [1.147(8)]
Fe–C3	1.834(3) [1.882(7)]	C4–O4	1.139(4) [1.14(1)]
Co–C2	1.943(3) [2.036(7)]	C5–O5	1.146(4) [1.127(8)]
Co–C3	2.225(3) [2.036(7)]	C6–O6	1.131(4) [1.127(8)]
Co–C4	1.801(3) [1.781(9)]	Fe–C(Cp*)	2.100(3)–2.147(3) [b]
Co–C5	1.771(4) [1.783(7)]	C–C(Cp*)	1.413(4)–1.440(4) [c]
Co–C6	1.802(4) [1.783(7)]	C–Me(Cp*)	1.493(5)–1.506(4)
Bond angles (°)			
Co–Fe–C2	48.21(9) [52.2(2)]	Co–C2–O2	138.9(2) [134.6(6)]
Co–Fe–C3	57.4(1) [52.2(2)]	Fe–C2–O2	137.5(2) [144.5(6)]
C2–Fe–C3	101.0(1) [96.8(3)]	Co–C3–Fe	78.7(1) [80.9(3)]
Fe–Co–C2	48.14(8) [46.9(2)]	Co–C3–O3	128.0(2) [134.6(6)]
Fe–Co–C3	43.95(8) [46.9(2)]	Fe–C3–O3	153.3(3) [144.5(6)]
C2–Co–C3	88.4(1) [87.5(3)]	C–C–C(Cp*)	107.6(3)–108.7(3) [d]
Co–C2–Fe	83.7(1) [80.9(3)]	C–C–Me(Cp*)	124.9(3)–126.4(3)

[a] Values in brackets are for the Cp analogue **15**. [b] [2.03(1)–2.08(1) Å]. [c] [1.29(2)–1.34(2) Å]. [d] [*ca.* 107°].

C–O: 134.6(6)°]. However, in the case of the Cp* complex **14**, lack of such symmetry causes differentiation of the two CO ligands. Namely, the C2O2 ligand is coordinated to Fe and Co in an essentially symmetrical manner as is evident from the similar M–C2 distances [1.941 (3) Å (Fe); 1.943(3) Å (CO)] as well as the similar M–C2–O2 angles [137.5(2)° (Fe); 138.9(2)° (CO)], whereas the C3O3 ligand is bonded more strongly to Fe than to Co [1.834(3) Å (Fe); 2.225(3) Å (Co)] and the O3 atom is tilted toward Co[Fe–C3–O3 = 153.3(3)°; Co–C3–O3 = 128.0(2)°]. The values for **14** are approximately equal to the averaged ones for **15** [Fe–C: 1.888 Å; Co–C: 2.084 Å; Fe–C–O: 145.4°; < Co–C–O: 133.5°].

The mechanisms of formation of the above-mentioned photolysis and thermolysis products, which are completely different from the decarbonylated products (**10**) of the analogues **9** (Scheme 3) have not been clear until now, because little information on intermediates and byproducts except for the detection of Fp_2(Fp_2^*) or **14** (**15**) has been available. However, formation of the photolysis product **11** may be explained by formal addition of a "(CP)FeCo$(CO)_4$" fragment to **10** (R=H) and its Cp* analogue which may be generated according to Scheme 3, although **10** (R=H) has never been detected at all. Such a cluster expansion reaction has been recognized as a general synthetic method for higher-nuclearity cluster compounds [17], and the (CP)FeCo$(CO)_4$ species may be generated by decarbonylative decomposition of **3** and, in the case of the thermolysis, (CP)FeCo$(CO)_6$**14** and **15** were actually isolated from the reaction mixture. Furthermore, coupling of the residual Co(C_2H) species and picking up of Co_2 fragments could explain the formation of **13**. In the case of the reaction of **3b**, the fate of the C_2H ligand cannot be determined by NMR and GLC analyses. The C_2 complex **4** decomposed upon thermolysis to give a mixture containing **2**.

2.3. Reduction of 3 with hydrosilanes

In addition to the study on polymetallic C_2H_n complexes, reduction of hydrocarbyl ligands in transition metal complexes by employing hydrosilane as an equivalent for H_2 is another subject of our study through which we hope to get information on the reduction step of surface-bound intermediates [18].

Reaction of **3a** with hydrosilanes [$HSiR_3$: R_3 = Me_3 (**a**), Et_3 (**b**), Me_2Et (**c**), Me_2Ph (**d**)] readily proceeded at ambient temperature to give a mixture of products containing 1,2-disilylethylene (**16a–d**) together with **12**, **15** and Fp_2 (eqn. (7)). Fig. 6 shows the ^{1}H-NMR spectrum of a reaction mixture of $HSiEt_3$.

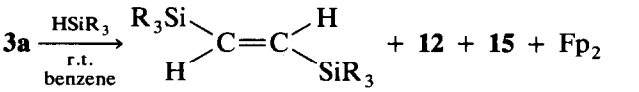

16

$(R_3 = Et_3)$ (73%) (22%) (74%) (8%)

(7)

The reduction products were identified by comparison of the NMR and GCMS data with those of authentic samples (**16a–c**) [19] or isolated by column chro-

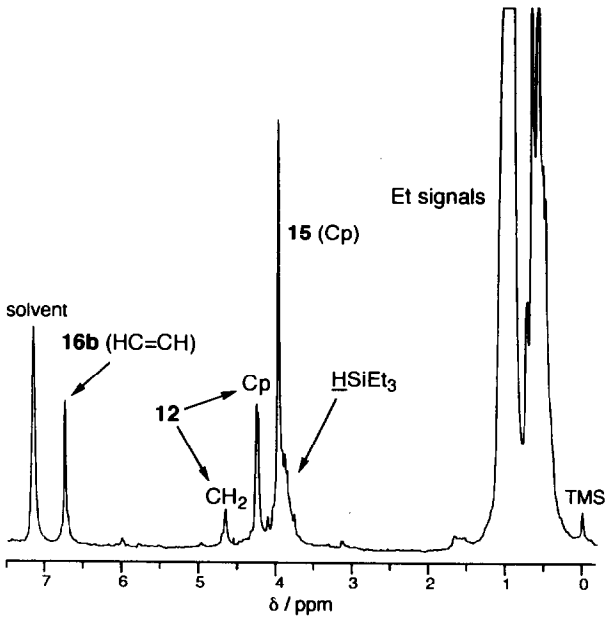

Fig. 6. ^{1}H-NMR spectrum (90 MHz) of a reaction mixture of **3a** and 3 equiv $HSiEt_3$ in C_6D_6 (r.t., 3 h). The Cp signal of Fp_2 appeared as a small shoulder peak of the Cp signal of **12**.

matography (**16d**), and they were readily detected by the singlet olefinic proton signals [δ_H (C_6D_6) 6.76 (**16a**), 6.74 (**16b**), 6.78 (**16c**), 6.83 (**16d**)] of reaction mixtures. Because C_2 ligands in polymetallic complexes frequently escaped from ^{13}C-NMR detection [1d,15] and the CH_2 signal of **12** could not be located by measurement at room temperature, the structures of **12** and **15** were characterized by spectroscopic methods and crystallography to be the vinylidene cluster with the butterfly $FeCo_3$ array, $CpFeCo_3(\mu_4$-C=$CH_2)C(CO)_9$, and the simple Fe–Co dimer, $CpFe(CO)(\mu$-$CO)_2Co(CO)_3$, respectively. The crystal structures of both the complexes were reported already (see above). The cell parameters of our products [**12**:*a* = 8.283(2), *b* = 18.120(3), *c* = 12.876(3) Å; orthorhombic; space group *Pbcm* [11]; **15**: *a* = 8.625(2), *b* = 10.952(2), *c* = 7.015(1) Å, *b* = 104.64(2)°; monoclinic; space group $P2_1/m$ [16a]] coincided with the reported values within experimental error, and the *R* values converged below 0.05 in both cases. On the basis of these assignments, the product distribution of the reaction with $HSiEt_3$ was estimated by ^{1}H-NMR as shown in eqn. (7). It was difficult to get reproducible isolated yields, because the highly labile Co-containing products suffered severe decomposition during chromatographic separation. **3b** also reacted with hydrosilanes in a manner similar to **3a** to give **16** and **14**. However, to our surprise, the tetranuclear C_2 complex **4** was totally inert toward hydrosilanes. This result supports the associative mechanism proposed for the fluxional behaviour of **4** [1d].

To consider the mechanism of formation of **16**, a couple of experiments were conducted. Treatment of **3a** with $DSiMe_3$ gave the dideuterated product **16a**-d_2 as confirmed by ^{1}H-NMR and GCMS analyses of the reaction mixture. This result implicated that the C=C moiety in **16** might result from deoxygenative coupling of two CO molecules induced by hydrosilanes [20]. The viability of this mechanism was checked by the reaction of the ^{13}CO-enriched **3a** (see above) with $HSiMe_3$. However, ^{13}C was not incorporated into **16a** at all as confirmed by GCMS analyses. These labeling experiments therefore indicated that the C=C moiety in **16** came from the C_2H ligand in **3a**, similar to the results of the reduction of **5** and (μ-η^2:η^2-Ph–C≡C–Ph)$Co_2(CO)_6$ giving hydrosilylated products, *i.e.* a mixture of two isomers $Ph(H)C{=}C(H)SiR_3$ and $CH_2{=}C(Ph)SiR_3$, and $Ph(H)C{=}C(Ph)SiR_3$, respectively. The former reaction also produced $CpFeCo_3(\mu_4$-C=CHPh)$(CO)_9$ (**17**), the Ph analogue of **15**.

Since the methylene hydrogen atoms in **12** obtained by the reaction with $DSiMe_3$ were not completely deuterated as in the case of **16**, these two products are expected to be formed by different reaction pathways. Although, in this case, too, the reaction mechanisms have remained unknown so far, **16** may arise from hydrosilylation of the C_2H functional group giving a $R_3Si(H)C{=}C(H)$–M intermediate followed by silylative cleavage of the C–M bond. At the present time, we have no explanation for the perdeuteration of the olefinic hydrogen atoms in **16**. On the other hand, formation of **12** and **17** can be explained by hydrometallation of the C_2R functional groups in **3a** and **5** by an $HCo(CO)_n$ species, respectively, and metal–metal bond formation.

2.4. *Reaction of 3a with alkenes and phenylacetylene*

In contrast to the above-mentioned reactions, **3** sometimes exhibited reactivities similar to alkyne adducts. Reaction between (μ-η^2:η^2-R–C≡C–R)$Co_2(CO)_6$ and alkene, the so-called Pauson-Khand reaction [21], has been utilized for construction of cyclopentenone skeletons, and electron-rich alkenes have been revealed to be much more reactive. Although vinyl acetate, an electron-rich alkene, did not react with **3a** but was polymerized upon heating, and cyclopentene left **3a** unaffected, strained alkenes such as norbornene and norbornadiene readily reacted with **3a** to give adducts **18** in moderate to good yields together with small amounts of **15**, $Co_4(CO)_{12}$ and Fp_2 (eqn. (8)).

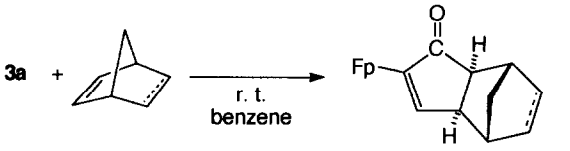

(8)

18a (from norbornene) : 98 %
18b (from norbornadiene) : 43 %

In the case of the reaction with norbornadiene (nbd), the Co residue was trapped as $Co_2(CO)_4(\eta^4$-nbd$)_2$ [22]. Because it was difficult to locate the very weak > C=O signals (^{13}C-NMR) of **18**, the molecular structure of

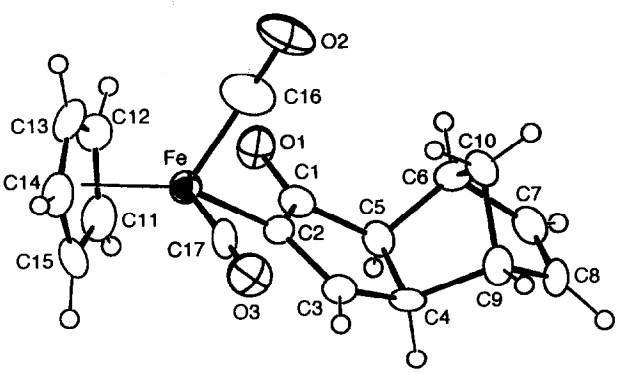

Fig. 7. Molecular structure of **18b** drawn at the 30% probability level.

TABLE 5. Selected structural parameters for **18b**.

Bond lengths (Å)			
FE-C2	1.94(1)	C4-C9	1.55(1)
Fe-C16	1.77(1)	C5-C6	1.53(1)
Fe-C17	1.73(1)	C6-C7	1.51(2)
C1-O1	1.24(1)	C6-C10	1.56(1)
C1-C2	1.52(1)	C7-C8	1.32(2)
C1-C5	1.51(1)	C8-C9	1.47(2)
C2-C3	1.35(1)	C9-C10	1.56(1)
C3-C4	1.49(1)	C16-O2	1.13(1)
C4-C5	1.55(1)	C17-O3	1.18(1)
Bond angles (°)			
O1-C1-C2	124 (1)	C4-C5-C6	103.1(9)
O1-C1-C5	123 (1)	C5-C6-C7	106 (1)
Fe-C2-C1	123.8(8)	C5-C6-C10	101.9(9)
Fe-C2-C3	133.9(9)	C7-C6-C10	98 (1)
C2-C3-C4	119 (1)	C6-C7-C8-	108 (1)
C3-C4-C5	102.8(9)	C7-C8-C9	108 (1)
C3-C4-C9	115 (1)	C4-C9-C8	107 (1)
C5-C4-C9	103.1(9)	C4-C9-C10	100.5(9)
C1-C5-C4	103.8(9)	C8-C9-C10	100 (1)
C1-C5-C6	114 (1)	C6-C10-C9	92.3(9)

the norbornadiene adduct **18b** was determined by X-ray crystallography (Fig. 7 and Table 5) to be the expected tricyclic cyclopentenone derivative. The cyclopentenone ring was fused to the norbornene skeleton from the sterically less congested *exo*-side, and the Fp-substituent occupied the α-position of the cyclopentenone ring as usually observed for the reaction products of 1-alkyne.

Finally, **3a** was found to exhibit catalytic activity for cyclotrimerization of phenylacetylene giving a *ca.* 3:1 mixture of 1,2,4- and 1,3,5-isomers of triphenylbenzenes. After the reaction, the Fp-C≡C-H moiety in **3a** was replaced by the substrate to give (μ-η^2:η^2-Ph-C≡C-H)$Co_2(CO)_6$. Although alkyne adducts were reported also to catalyze the cyclotrimerization [3a], the initial reaction rate induced by **3a** was larger than that induced by the Ph-C≡C-H adduct. Ten equivalents of Ph-C≡C-H were consumed within 5 h at ambient temperature. This may result from the higher lability of CO ligands in **3a** as shown above. However, after a certain reaction time the catalytic activity became almost the same as that of the Ph-C≡C-H adduct owing to the ligand replacement reaction.

3. Conclusion

Of the μ-η^2:η^2-adducts of FP-C≡C-H (**1**) to Co_2, Ni_2 and Mo_2 species which we have prepared [1], the Co derivatives **3** exhibit the highest reactivity, reflecting the lability of the Co-CO bond [4]. However, because the resulting primary reaction products also contain highly labile Co-CO functional groups, only secondary

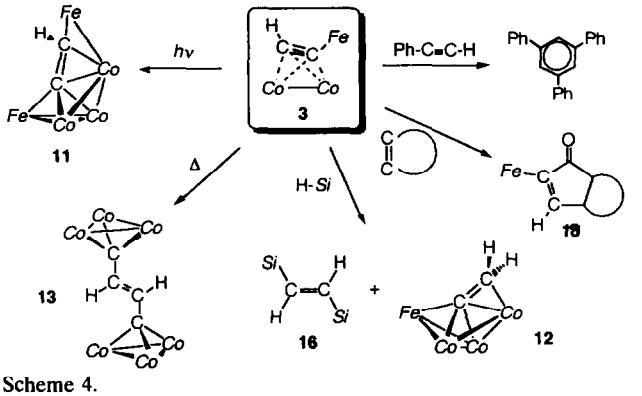

Scheme 4.

reaction products have been isolated and characterized. Although this limitation hinders clarification of the reaction mechanisms, the present study summarized in Scheme 4 (ligands are omitted for clarity) has revealed that the C_2H complexes **3** serve as building blocks for polynuclear complexes **11**–**13**. **11** and **12** are apparently formed by addition of a (CP)FeCo fragment to **3** and by hydrometallation of **3** by a $HCo(CO)_n$ species, respectively. It is also revealed that **3** shows reactivity similar to alkyne adducts with respect to Pauson-Khand reaction and catalytic cyclotrimerization of 1-alkyne.

4. Experimental details

4.1. General

All manipulations were carried out under argon by standard Schlenk tube techniques. Ether, THF, benzene and hexanes (Na-K alloy) and CH_2Cl_2(P_2O_5) were treated with appropriate drying agents, distilled, and stored under argon **3** and **4** were prepared according to the method described in our previous paper [1d]. Hydrosilanes **16a,b** were prepared by $LiAlH_4$ reduction of appropriate chlorosilanes in butyl ether or diglyme, and $Co_4(CO)_{12}$ was prepared by thermolysis of $Co_2(CO)_8$ according to [23]. Other chemicals were purchased and used as received. Column chromatography was performed on alumina [activity II ~ IV (Merck Art. 1097)] or silica gel [column: Kieselgel 60 (Merck Art. 7734); PTLC: Kieselgel 60 PF_{254} (Merck Art. 7747)].

^1H- and ^{13}C-NMR spectra were recorded on JEOL EX-90 (^1H: 90 MHz) and JEOL GX-270 spectrometers (^1H:270 MHz; ^{13}C: 67.9 MHz). Solvents for NMR measurements containing 1% TMS as an internal standard were dried over molecular sieves and distilled under reduced pressure. Coupling constants are expressed in Hz and unless otherwise stated are for $J(^{13}C-^1H)$. IR and GC- and FD-MS analyses were performed on a JASCO FT/IR 5300 spectrometer and

a Hitachi M-80 mass spectrometer, respectively. Photolysis was carried out by using a high pressure mercury lamp (USHIO UM-452).

4.2. ^{13}CO-exchange reaction of 3a

A benzene solution of **3a** pressurized by ^{13}CO (2 atm) in a glass autoclave was stirred overnight at room temperature. Removal of the volatiles gave the ^{13}CO-enriched **3a**.

4.3. Reaction of Fp–C≡C–R (R = H, Ph) with ^{13}CO-enriched $Co_2(CO)_8$

A benzene solution (10 ml) of $Co_2(CO)_8$ (342 mg, 1.00 mmol) pressurized by ^{13}CO (2 atm) in a glass autoclave was stirred overnight at ambient temperature. After incorporation of ^{13}CO was checked by IR, the dissolved ^{13}CO was removed by evacuation for a few minutes. Then Fp–C≡C–H (202 mg, 1.00 mmol) was added to the solution. The reaction proceeded with evolution of CO. The evolved CO dissolved in the solution phase was removed by evacuation to avoid exchange between the resulting **3a** formed and the evolved ^{13}CO. Work up as described for **3a** [1d] gave the ^{13}CO-enriched **3a**.

Similar treatment of Fp–C≡C–Ph gave a ^{13}CO-enriched sample of **5**.

4.4. Reaction of 3a with PPh_3

A benzene solution (2 ml) of **3a** (98 mg, 0.20 mmol) and PPh_3 (63 mg, 0.24 mmol) was stirred for 1.5 h at ambient temperature. Separation by preparative TLC (silica gel developed by ether/hexanes = 1/8) gave an orange band of **7**. An analytically pure sample could not be obtained due to thermal instability. **7**: ^{1}H-NMR (C_6D_6) δ 4.17 (5H, s, Cp), 5.53 (1H, d, $J(^1H-^{31}P) = 12$, C_2H); ^{13}C-NMR (C_6D_6) δ 87.6 (d, $J = 180.2$, Cp), 97.6 (dd, $J(^{13}C-^{31}P) = 3.7$, $J(^{13}C-^1H) = 209.6$, C≡*C*–H), 101.9 (dd, $J(^{13}C-^{31}P) = 7.3$, $J(^{13}C-^1H) = 11.0$, *C*≡C–H), 203.6 (br, Co–CO), 213.2 (br, Co–CO), 213.5 (d, $J_{P-C} = 23.9$, Fe–CO); ^{31}P-NMR (C_6D_6; external standard: phosphoric acid) δ 29.2; IR (KBr) ν(C≡O) 2041, 2012 and 1945 cm^{-1}; FD-MS 722 (M^+).

4.5. Photolysis of 3a

A benzene solution (60 ml) of **3a** (540 mg, 1.11 mmol) was irradiated with slow Ar purge for 40 h. After evaporation of the volatiles, the residue was extracted with ether and passed through an alumina pad. Recrystallization of the residue from ether/hexanes gave **11a** (130 mg, 0.18 mmol, 33% yield based on Fe) as black microcrystals. ^{1}H-NMR (CD_2Cl_2) δ 5.28 (5H, s, Cp), 5.40 (5H, s, Cp), 12.52 (1H, s, C=CH); ^{13}C-NMR (CD_2Cl_2 at −80°C) δ 89.1 (d, $J = 181.6$, Cp), 93.5 (d, $J = 180.1$, Cp), 187.3 (d, $J = 167.8$, C=*C*H), 196 (br, Co–CO), 209 (br, Co–CO), 212.8 (s, Fe-CO), 244.8 (s, μ-CO), 248 (br, μ-CO), 306.7 (s, *C* = CH); IR (KBr) ν(C≡O) 2051, 1985, 1953, 1849 and 1818 cm^{-1}; FDMS (M^+) 724; Anal. Calcd. for $C_{22}H_{11}O_{10}Fe_2Co_3$: C, 36.51; H, 1.52. Found C, 36.29; H, 1.69%.

4.6. Photolysis of 3b

A benzene solution (200 ml) of **3b** (1.13 g, 2.02 mmol) in a quartz Schlenk tube was irradiated with slow Ar purge for 18 h. After evaporation of the volatiles, the residue was extracted with CH_2Cl_2 and passed through an alumina pad. Recrystallization from ether/CH_2Cl_2 gave **11b** (570 mg, 0.66 mmol, 65% yield) as black microcrystals. ^{1}H-NMR ($CDCl_3$) δ 1.83 (15H, s, Cp*), 2.00 (15H, s, Cp*), 11.66 (1H, s, C=CH); ^{13}C-NMR ($CDCl_3$) δ 9.1 (q, $J = 128.2$, C_5Me_5), 9.4 (q, $J = 128.2$, C_5Me_5), 98.1 (s, C_5Me_5), 102.7 (s, C_5Me_5), 192.8 (d, $J = 162.0$, C=*C*H), 215.5 (s, Fe–CO), 248.8 (s, μ-CO), 253.1 (s, μ-CO), 310.0 (s, *C*=CH) (other CO's attached to Co could not be located); IR (KBr) ν(C≡O) 2041, 1997, 1957, 1823 and 1804 cm^{-1}; FDMS (M^+) 864; Anal. Calcd. for $C_{32}H_{31}O_{10}Fe_2Co_3$: C, 44.49; H, 3.59. Found C, 44.04; H, 3.12%.

4.7. Thermolysis of 3a

A benzene solution (20 ml) of **3a** (488 mg, 1.00 mmol) was heated in a glass autoclave for 18.5 h at 90°C. After removal of the volatiles under reduced pressure, the resulting residue was extracted with CH_2Cl_2 and passed through an alumina pad. The filtrate was separated by column chromatography (alumina). Purple band eluted with CH_2Cl_2/hexanes = 1/6 was collected and recrystallized from CH_2Cl_2/hexanes to give **13** (red-purple crystals, 48 mg, 0.07 mmol, 21% yield based on C_2H). ^{1}H-NMR ($CDCl_3$) δ 7.96 (2H, s, =CH–); ^{13}C-NMR ($CDCl_3$) δ 150.0 (d, J = 154.3, =CH–), 199.5 (s, Co–CO), 344.2 (s, CCo_3); IR (KBr) ν(C≡O) 2027 cm^{-1}; Anal. Calcd. for $C_{22}H_2O_{18}Co_6$: C, 29.10; H, 0.22. Found C, 28.99; H, 0.42%.

4.8. Thermolysis of 3b

A benzene solution (30 ml) of **3b** (800 mg, 1.30 mmol) was heated in a glass autoclave for 16 h at 70°C. After evaporation of the volatiles the residue was extracted with CH_2Cl_2 and recrystallized from CH_2Cl_2/hexanes to give **11b** (51 mg). The supernatant was then separated by alumina column chromatography eluted with CH_2Cl_2/hexanes mixed solvent. **14** (111 mg, 0.266 mmol, 20% yield) was isolated as dark brown crystals from orange band. A dark grey band contained **11b** (36

mg, combined yield: 87 mg, 0.10 mmol, 15% based on Fe). **14**: ^{1}H-NMR ($CDCl_3$) δ 1.81 (s, Cp*); ^{13}C-NMR (CD_2Cl_2) δ 9.1 (q, J = 128.5, C_5Me_5), 98.5 (s, C_5Me_5), 218.8 (br, CO); IR (KBr) ν(C≡O) 2050, 1988, 1958, 1858 and 1776 cm^{-1}.

4.9. Reaction of 3a with $HSiEt_3$: Isolation of 12 and 15

To a benzene solution (25 ml) of **3a** (1.06 g, 2.17 mmol) was added $HSiEt_3$ (1.04 ml, 6.52 mmol), and the mixture was stirred for 1 h at room temperature. After removal of the volatiles under reduced pressure, the residue was extracted with CH_2Cl_2 and passed through a silica gel pad. Separation by column chromatography (silica gel) gave a brown band (eluted with CH_2Cl_2 : hexanes = 1 : 8 → 1 : 7) and a dark brown band (eluted with CH_2Cl_2 : hexanes = 1 : 7), from which **12** (40 mg, 0.07 mmol, 6% yield) and **15** (23 mg, 0.06 mmol, 3% yield) of X-ray quality were isolated after repeated recrystallization from CH_2Cl_2-hexanes. Further elution with CH_2Cl_2 : hexanes = 1 : 2 gave Fp_2 (220 mg). **12** and **15** were identified by comparison of the ^{13}C-NMR (for **12** at −80°C) and crystallographic data with those reported.

4.10. Reaction of 3a with $HSiMe_2Ph$: isolation of 16d

3a (488 mg, 1.00 mmol) and $HSiMe_2Ph$ (0.46 ml, 3.0 mmol) were allowed to react for 1 h as described above. Separation by column chromatography gave a purple band eluted with CH_2Cl_2 : hexanes = 1 : 10. Crystallizations from hexanes and then from ether followed by sublimation gave colourless crystals of **16d** (56 mg, 0.19 mmol, 19% isolated yield). **16d**: ^{1}H-NMR (C_6D_6) δ 0.33 (s, 12H, s, $SiMe_2$ × 2), 6.83 (2H, s, CH=CH), 6.9–7.5 (10H, m, Ph × 2). ^{13}C-NMR ($CDCl_3$) δ −2.9 (qd, J = 119.8 and 1.5, SiMe), 127.8 (d, J = 158.7, Ph), 128.9 (d, J = 152.3, Ph), 133.9 (d, J = 154.9, Ph), 138.6 (s, Ph), 150.4 (d, J = 138.9, CH=CH). Anal. Calcd. for $C_{18}H_{24}Si_2$: C, 72.90; H, 8.16. Found C, 73.01; H, 8.20%.

4.11. Reaction of 5 with $HSiMe_2Et$: isolation of 17

5 (1.00 g, 1.77 mmol) and $HSiMe_2Et$ (0.59 ml, 5.32 mmol) were allowed to react in benzene (30 ml) for 1.5 h at room temperature. Work up as described above and chromatographic separation gave **15** (142 mg; eluted with CH_2Cl_2 : hexanes = 1 : 6 → 1 : 3) and **17** (31 mg, 0.05 mmol, 5% yield). **17**: ^{1}H-NMR (C_6D_6) δ 4.33 (5H, s, Cp), 5.13 (1H, s, C*H*Ph), 6.8–7.2 (5H, m, Ph). ^{13}C-NMR (CD_2Cl_2 at −80°C) δ 82.2 (d, J = 158.1, C*H*Ph), 94.0 (d, J = 182.0, Cp), 297.3 (s, *C*=CHPh), Ph and CO signals were observed around 130 (Ph), 200 (*CO*), 250 (μ-*CO*) ppm, respectively. FD-MS (M^+) 652. Anal. Calcd. for $C_{22}H_{11}O_9FeCo_3$: C, 40.53; H, 1.70. Found C, 40.26; H, 1.43%.

4.12. Reaction of 3a with norbornene

A benzene solution (5 ml) of **3a** (488 mg, 1.00 mmol) and norbornene (188 mg, 2.00 mmol) was stirred for 2.5 h at room temperature. After evaporation of the volatiles, the residue was extracted with CH_2Cl_2 and passed through a silica gel pad. Products were separated by column chromatography (silica gel). Elution with CH_2Cl_2/hexanes = 1/3 → 3/1 gave $Co_4(CO)_{12}$ (purple-black band, 58 mg, 0.10 mmol) and then Fp_2 (red-brown band, 40 mg, 0.11 mmol). Further elution with CH_2Cl_2 gave **18a** (yellow band, 320 mg, 0.98 mmol, 98% yield), which was isolated as an orange solid after recrystallization from ether/hexanes. ^{1}H-NMR (C_6D_6) δ (norbornyl protons) 0.75 (1H, d, J = 9.9), 1.02 (2H, s), 1.05 (2H, s), 1.36 (1H, m), 1.90 (1H, s), 2.06 (1H, d, J = 5.3), 2.41 (1H, dd, J = 2.6 and 5.0), 2.50 (1H, s); 4.25 (5H, s, Cp), 7.27 (1H, d, J = 2.6, CH); ^{13}C-NMR (C_6D_6) δ 28.8, 29.0, 31.3, 39.1, 39.6, 52.9, 53.6 (norbornyl skeleton), 85.7 (d, J = 181.7, Cp), 173.6 (d, J = 159.5, =CH), 216.2 (s, Fe–CO), 216.4 (s, Fe–CO) (C=O carbon could not be located.); IR (CH_2Cl_2) ν(C≡O) 2022, 1967 and ν(C=O) 1668 cm^{-1}; Anal. Calcd. for $C_{17}H_{16}O_3Fe$: C, 62.99; H, 4.98. Found C, 62.76; H, 5.07%.

4.13. Reaction of 3a with norbornadiene

A benzene solution (2.5 ml) of **3a** (244 mg, 0.50 mmol) and norbornadiene (0.15 ml, 0.15 mmol) was stirred for 100 min at room temperature. After evaporation of the volatiles, the residue was dissolved in CH_2Cl_2 and passed through a silica gel pad. Recrystallization from CH_2Cl_2/hexanes gave $Co_2(CO)_4(\eta^4$-nbd$)_2$ (146 mg, 0.353 mmol, 71% yield). Separation of the supernatant by column chromatography as described for **18a** gave $Co_4(CO)_{12}$ (11.9 mg, 0.02 mmol) and **18b** (yellow crystals after recrystallization from ether/hexanes, 70 mg, 0.22 mmol, 43% yield). ^{1}H-NMR ($CDCl_3$) δ (norbornenyl protons) 1.25 (1H, d, J = 8.9), 1.34 (1H, d, J = 8.9), 2.25 (1H, d, J = 5.3), 2.39 (1H, s), 2.57 (1H, m), 3.00 (1H, s), 5.99 (2H, m); 4.24 (5H, s, Cp), 7.30 (1H, d, J = 2.6, CH); ^{13}C-NMR ($CDCl_3$) δ 41.7, 44.2, 44.5, 51.5, 53.1 (norbornenyl skeleton), 85.0 (d, J = 179.6, Cp), 137.8, 137.8 (norbornenyl skeleton), 156.4 (s, Fe–C), 174.3 (d, J = 159.5, =CH), 213.8 (s, C=O), 216.0 (s, Fe–CO), 216.2 (s, Fe–CO); IR (CH_2Cl_2) ν(C≡O) 2023, 1967 and ν(C=O) 1671 cm^{-1}; Anal. Calcd. for $C_{17}H_{14}O_3Fe$: C, 63.38; H, 4.38. Found C, 63.49; H, 4.65%.

4.14. X-ray crystallography of 11a, 13, 14 and 18b

11a, **13**, **14** and **18b** were recrystallized from CH_2Cl_2-hexanes and ether-hexanes mixed solvent systems, respectively, and suitable crystals were mounted on glass fibres. Diffraction measurements were made

on Rigaku AFC5 (**11a**) and AFC-5R (**13, 14, 18b**) automated four-circle diffractometers by using graphite-monochromated Mo Kα radiation ($\lambda = 0.71059$ Å). The unit cells were determined and refined by a least-squares method using 20–24 independent reflections. Data were collected with an ω-2θ scan technique. If $\sigma(F)/F$ was more than 0.1, a scan was repeated up to three times and the results were added to the first scan. Three standard reflections were monitored at every 150 measurements. All data processing was performed on a Micro Vax II computer or an Iris Indigo computer with the TEXSAN program (Rigaku, Tokyo). Neutral scattering factors were obtained from the standard source [24]. In the reduction of data, Lorentz, polarization, and empirical absorption corrections (Ψ scan) were made.

The structures were solved by a combination of direct methods (SAPI91 or MITHRIL) and Fourier synthesis (DIRDIF). All the non-hydrogen atoms were refined anisotropically. All the hydrogen atoms except for H2 of **13** were fixed at the calculated positions (C–H = 0.95 Å) and were not refined. H2 of **13** was refined isotropically. The crystallographic data and selected structural parameters are summarized in Tables 1–5. Tables of positional, anisotropic thermal and full structural parameters and structure factors are available from the first author.

Acknowledgment

This work was supported by the Grant-in-Aid for Scientific Research on Priority Area from the Ministry of Education, Science and Culture, Japan (No. 04241105 & 05236103).

References

1 (a) M. Akita, M. Terada, S. Oyama and Y. Moro-oka, *Organometallics, 9* (1990) 816; (b) M. Akita, M. Terada, S. Oyama, S. Sugimoto and Y. Moro-oka, *Organometallics, 10* (1991) 1561; (c) M. Akita, M. Terada and Y. Moro-oka, *Organometallics, 10* (1991) 2962; (d) M. Akita, M. Terada and Y. Moro-oka, *Organometallics, 11* (1992) 1825; (e) M. Akita, M. Terada and Y. Moro-oka, *Organometallics, 11* (1992) 3468; (f) M. Akita, S. Sugimoto, M. Tanaka and Y. Moro-oka, *J. Am. Chem. Soc., 114* (1992) 7581; (g) M. Akita, S. Sugimoto, M. Terada and Y. Moro-oka, *J. Organomet. Chem., 447* (1993) 103; (h) M. Akita, S. Sugimoto, A. Takabuchi, M. Tanaka and Y. Moro-oka, *Organometallics, 12* (1993) 2925; (i) M. Akita, N. Ishii, A. Takabuchi, M. Tanaka and Y. Moro-oka, *Organometallics, 13* (1994) 258.

2 (a) E. Sappa, A. Tiripicchio and P. Braunstein, *Chem. Rev., 83* (1983) 203; (b) P.R. Raithby and M.J. Rosales, *Adv. Inorg. Chem. Radiochem., 29* (1985) 169; (c) R. Nast, *Coord. Chem. Rev., 47* (1982) 89.

3 Co: (a) R.S. Dickson and P.J. Fraser, *Adv. Organomet. Chem., 12* (1974) 323; Ni: (b) J.F. Tilney-Bassett and O.S. Mills, *J. Am. Chem. Soc., 81* (1959) 4757; (c) P.W. Jolly and G. Wilke, *The Organic Chemistry of Nickel*, Academic Press, New York, 1974, Vol. 1; Mo: (d) A. Nakamura and N. Hagihara, *Nippon Kagaku Zasshi, 84* (1963) 344; (e) W.I. Baily, Jr., M.H. Chisolm, F.A. Cotton and L.A. Rankel, *J. Am. Chem. Soc., 100* (1978) 5764; (f) M.D. Curtis, *Polyhedron, 6* (1987) 759. See also, (g) M.J. Winter, *Adv. Organomet. Chem., 29* (1989) 101 and references cited therein.

4 (a) G. Cetini, O. Gambino, P.L. Stanghellini and G.A. Vaglio, *Inorg. Chem., 6* (1967) 1225; (b) S. Aime, L. Milone, R. Rosetti and P.L. Stanghellini, *Inorg. Chim. Acta, 22* (1977) 135.

5 (a) K. Wade, *Adv. Inorg. Radiochem., 18* (1976) 1; (b) D.M.P. Mingos, *Acc. Chem. Res., 17* (1984) 311; (c) S.M. Owen, *Polyhedron, 7* (1988) 253.

6 L.S. Chia, W.R. Cullen, M. Franklin and A.R. Manning, *Inorg. Chem., 14* (1975) 2521.

7 K. Yasufuku and H. Yamazaki, *Bull. Chem. Soc. Japan, 45* (1972) 2664.

8 M.I. Bruce, D.N. Duffy and M.G. Humphrey, *Aust. J. Chem., 39* (1986) 159.

9 A.J. Carty, A.A. Cherkas and L.H. Randall, *Polyhedron, 7* (1988) 1045.

10 E. Sappa, A. Tiripicchio, A.J. Carty and G.E. Toogood, *Prog. Inorg. Chem., 35* (1987) 437.

11 P. Brun, G.M. Dawkins, M. Green, R.M. Mills, J.-Y. Salaün, F.G.A. Stone and P. Woodward, *J. Chem. Soc., Dalton Trans.*, (1983) 1357.

12 L.F. Dahl and D.L. Smith, *J. Am. Chem. Soc., 84* (1962) 2450.

13 B.R. Penfold and B.H. Robinson, *Acc. Chem. Res., 6* (1973) 73.

14 J. March, *Advanced Organic Chemistry* (3rd ed.), Wiley-Interscience, New York, 1985, p. 19.

15 T. Weidman, V. Weinrich, B. Wagner, C. Robl and W. Beck, *Chem. Ber., 124* (1991) 1363.

16 (a) I.L.C. Campbell and F.S. Stephens, *J. Chem. Soc., Dalton Trans.*, (1975) 22; (b) T. Madach and H. Vahrenkamp, *Chem. Ber., 113* (1980) 2675.

17 D.F. Shriver, H.D. Kaesz and R.D. Adams (eds.), *The Chemistry Metal Cluster Complexes*, VCH, New York, 1990.

18 (a) M. Akita, O. Mitani, M. Sayama and Y. Moro-oka, *Organometallics, 10* (1991) 1394; (b) M. Akita, T. Oku, M. Tanaka and Y. Moro-oka, *Organometallics, 10* (1991) 3080; (c) M. Akita, T. Oku and Y. Moro-oka, *J. Chem. Soc., Chem. Commun.*, (1992) 1031; (d) M. Akita, T. Oku, R. Hua and Y. Moro-oka, *J. Chem. Soc., Chem. Commun.*, (1993) 1670.

19 (a) L. Birkofer and T. Kühn, *Chem. Ber., 111* (1978) 3119; (b) J.-P. Pillot, J. Donogués and R. Calas, *Bull. Chim. Soc. Fr.*, (1975) 2143; (c) Synthesis, (1977) 479. (d) H. Matsumoto, S. Nagashima, T. Kato and Y. Nagai, *Angew. Chem. Int. Ed. Engl., 17* (1978) 279.

20 See, for example: (a) P.T. Wolczanski and J.E. Bercaw, *Acc. Chem. Res., 13* (1980) 21; (b) E.M. Carnahan, J.D. Protasiewicz and S.J. Lippard, *Acc. Chem. Res., 26* (1993) 90; (c) C.C. Cummins, G.D. Van Duyne, C.P. Shaller and P.T. Wolczanski, *Organometallics, 10* (1991) 164; (d) references cited in 18 (a–c).

21 P.L. Pauson, in A. de Meijere and H. tom Dieck (eds.), *Organometallics in Organic Synthesis*, Springer, Berlin Heidelberg, 1988, p. 233.

22 (a) G. Winkhaus and G. Wilkinson, *J. Chem. Soc.*, (1961) 602; (b) P. McArdle and A.R. Manning, *J. Chem. Soc. (A)*, (1970), 2123.

23 T. Eguchi, H. Nagayama, H. Ohki, S. Takeda, N. Nakamura, S. Kernaghan and B.T. Heaton, *J. Organomet. Chem., 428* (1992) 207.

24 *International Tables for X-ray Crystallography*, Vol. 4, Kynoch Press, Birmingham, 1975.